BIOCHEMISTRY
including biophysical chemistry & molecular biology

Rapid Report

pubs.acs.org/biochemistry

The Influenza A PB1-F2 and N40 Start Codons Are Contained within an RNA Pseudoknot

Salvatore F. Priore, Andrew D. Kauffmann, Jayson R. Baman, and Douglas H. Turner*

Department of Chemistry and Center for RNA Biology, University of Rochester, Rochester, New York 14627, United States

Supporting Information

ABSTRACT: Influenza A is a negative-sense RNA virus with an eight-segment genome. Some segments encode more than one polypeptide product, but how the virus accesses alternate internal open reading frames (ORFs) is not completely understood. In segment 2, ribosomal scanning produces two internal ORFs, PB1-F2 and N40. Here, chemical mapping reveals a Mg^{2+}-dependent pseudoknot structure that includes the PB1-F2 and N40 start codons. The results suggest that interactions of the ribosome with the pseudoknot may affect the level of translation for PB1-F2 and N40.

Influenza A is a negative-sense RNA virus composed of eight discrete segments. Influenza infections are predicted to cause 25000 deaths annually in the United States.[1] The possibility of pandemic influenza strains, illustrated by the recent H5N1 and H7N9 outbreaks, makes this virus a public health concern.[2,3] While each segment of influenza A virus encodes a main protein product, segments 2, 3, and 7 and 8 also encode additional polypeptide products by ribosomal scanning, ribosomal frameshifting, and alternative splicing, respectively.[4−7] Segment 2 (PB1) encodes the alternative polypeptide products PB1-F2 and N40, the former acting as a pro-apoptotic factor and the latter of unknown function.[8,9] While ribosomal scanning past the main PB1 start codon is responsible for accessing the internal PB1-F2 and N40 open reading frames (ORFs), there may be other factors that control initiation at the proper start codon.

RNA secondary structure is a well-known mechanism for facilitating noncanonical translation. For example, frameshifting pseudoknots or internal ribosome entry sites (IRES) represent structured RNA domains that provide alternative ORFs by causing the translating ribosome to "slip" backward or bypass standard cap-dependent translation initiation by serving as an internal ribosome binding domain, respectively.[10,11] To search for potential secondary structures containing the start codons for PB1-F2 and N40, a consensus sequence was derived for the local region. When the program DotKnot[12] was used to scan the consensus sequence, a conserved pseudoknot was predicted. Base pairing frequencies determined from an alignment of all available unique influenza sequences for this region are consistent with this folding but revealed no compensatory changes (see Figure 11 of ref 16). Computations of pseudoknots in biologically relevantly sized sequences without any chemical mapping or phylogenetic data predict as few as 5% of pseudoknotted base pairs correctly.[13] Here, chemical mapping in vitro with NMIA, DMS, and CMCT[14] is shown to be consistent with the possible pseudoknot, and the folding is found to depend on Mg^{2+} (Figure 1). As a reminder, NMIA modifies the ribose 2′-OH group of flexible (single-stranded) nucleotides; DMS modifies the pairing faces of single-stranded A's and C's, while CMCT similarly modifies U's. All chemical mapping data can be found in the SNRNASM database (see the methods section of the Supporting Information).

The absence of significant chemical modification at positions 65−69 and 102−106 in the presence of Mg^{2+} is consistent with a pseudoknotted helix at these positions. Moreover, when the NMIA data were incorporated into ShapeKnots, the model in Figure 1 was predicted to be the most stable conformation. The topology of this pseudoknot is unusual because the pseudoknotted helices are not coaxially stacked on each other.

An important characteristic of pseudoknots is their dependence on multivalent cations, such as Mg^{2+}, to stabilize their formation.[20] As shown in Figure 1, there are important differences between chemical reactivity in the presence and absence of Mg^{2+}. In particular, increased chemical reactivity at positions 69, 86, 101, and 107 in the absence of Mg^{2+} indicates destabilization of the folded RNA. Approximate initial melting temperatures determined with UV absorbance were 53 and 72 °C in the absence and presence of Mg^{2+}, respectively, and the melting curve in the presence of Mg^{2+} suggests an additional transition above 95 °C (Figure S1 of the Supporting Information). These results further indicate that Mg^{2+} stabilizes the pseudoknot. No cooperative structural changes could be observed at 37 °C, thus indicating that the structure is completely folded under the conditions used for chemical mapping experiments.

To further investigate the folding of this RNA, two sets of mutant sequences predicted to disrupt and rescue either of the pseudoknotted helices were synthesized. Chemical mapping reveals that the sequence in Figure 2A disrupts helix 1, as demonstrated by increased chemical reactivity at nucleotides 69 and 103−106 in the presence of Mg^{2+}. Compensatory mutations to restore helix 1 provide protection to nucleotides 69 and 103−106, but only in the presence of Mg^{2+} (Figure 2B). These results are consistent with formation of a pseudoknot.

The sequence in Figure 2C is predicted to destabilize helix 2 by reversing the orientation of nucleotides 93−97. This is confirmed by increased chemical reactivity for nucleotides 116,

Received: December 30, 2014
Revised: May 19, 2015
Published: May 21, 2015

DOI: 10.1021/bi501564d
Biochemistry 2015, 54, 3413−3415

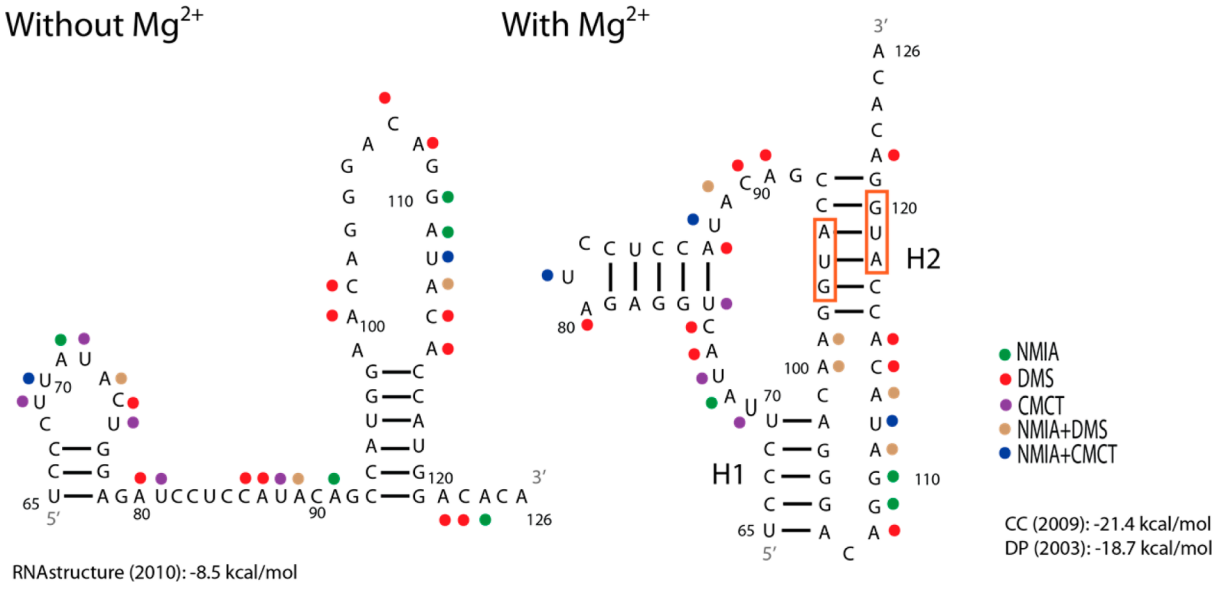

Figure 1. Structural models of the influenza A segment 2 (PB1) region of nucleotides 65−126. To optimize the SP6 polymerase efficiency, the identities of nucleotides 63 and 64 (not shown) are both A's; however, in the wild-type sequence, the nucleotides are A and U, respectively. The structure without Mg^{2+} is predicted with RNAstructure,[15] in which strongly reactive nucleotides were forced to be single-stranded. The structure shown in the presence of Mg^{2+} is the one most consistent with the model based on a comparison of sequences.[16] This structure is also predicted by ShapeKnots.[17] The predicted free energy at 37 °C for the structure without Mg^{2+} is reported at the bottom left.[15] Predicted free energies at 37 °C from two pseudoknot prediction models are reported at the bottom right.[18,19] Red boxes indicate the start codons for PB1-F2 and N40 ORFs, respectively. Colored dots represent strong chemical mapping hits for the reagent identified in the key. H1 denotes helix 1 and H2 helix 2.

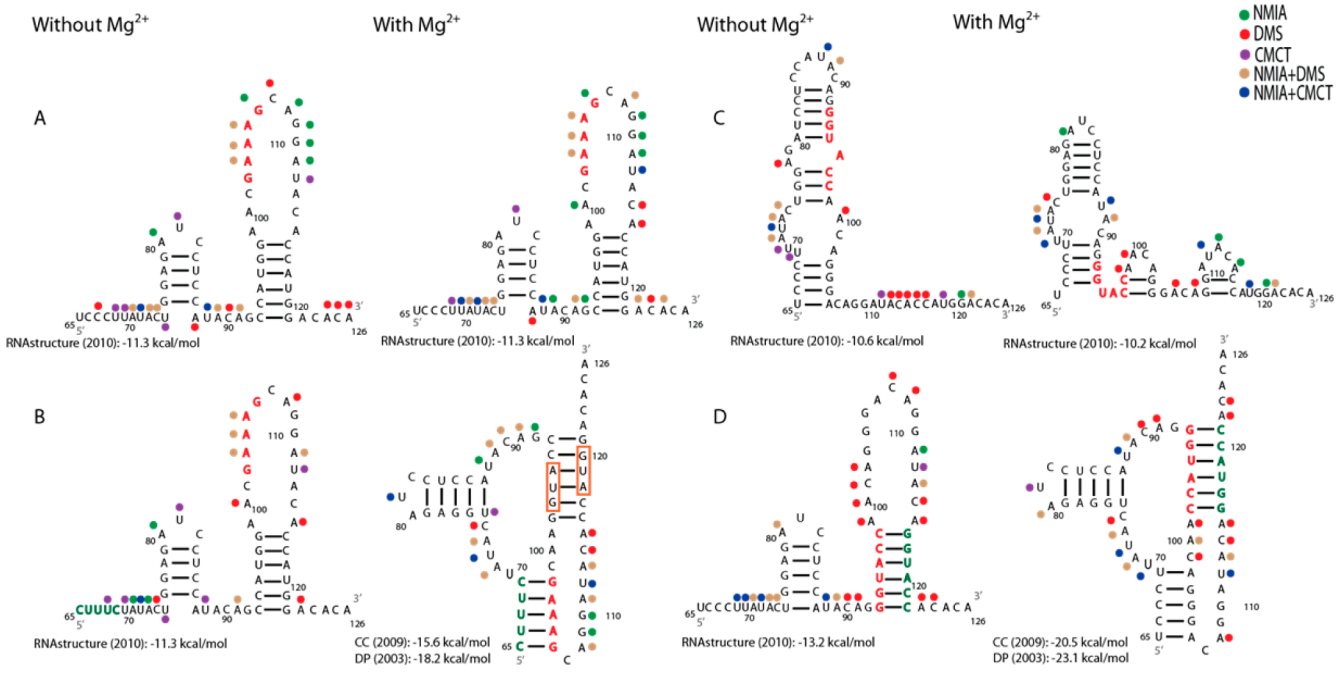

Figure 2. Chemical mapping results for four mutant sequences with and without Mg^{2+}. Red nucleotides indicate predicted destabilizing nucleotide changes and green nucleotides compensatory changes. Predicted nonpseudoknotted structures were modeled with RNAstructure as in Figure 1. Predicted pseudoknotted structures (panels B and D, with Mg^{2+}) were previously modeled with ShapeKnots and overlaid with chemical mapping results. (A) Destabilizing mutant sequence for helix 1. (B) Compensatory mutant sequence for helix 1. (C) Destabilizing mutant sequence for helix 2. (D) Compensatory mutant sequence for helix 2. Other figure annotations are as in Figure 1.

117, 119, and 121 in the absence of Mg^{2+} and 119 and 121 in the presence of Mg^{2+}. When the orientations of nucleotides 115−120 are also reversed to restore base pairing, the nucleotides of helix 2 are protected from chemical modification (Figure 2D). The resulting reactivity pattern in the presence of Mg^{2+} is similar to those shown in Figures 1 and 2B, consistent with the proposed pseudoknot model.

Chemical mapping experiments of the native, destabilized, and compensatory mutant sequences strongly favor formation of a pseudoknot at nucleotides 65−126 of influenza A segment 2, which contains the PB1-F2 and N40 start sites. The results

DOI: 10.1021/bi501564d
Biochemistry 2015, 54, 3413−3415

suggest a structural role of this pseudoknot in regulating translation initiation and therefore expression of PB1-F2 and N40. In light of PB1-F2 pro-pathogenic characteristics, this pseudoknot may provide a target for rational drug design.

■ ASSOCIATED CONTENT

Supporting Information

Detailed materials and methods. The Supporting Information is available free of charge on the ACS Publications website at DOI: 10.1021/bi501564d.

■ AUTHOR INFORMATION

Corresponding Author

*E-mail: turner@chem.rochester.edu. Telephone: (585) 275-3207.

Author Contributions

S.F.P. and A.D.K. contributed equally to this work.

Funding

This work was supported by National Institutes of Health Grant R01 GM022939. S.F.P. is a trainee in the MSTP program supported by Grant T32 GM007356.

Notes

The authors declare no competing financial interest.

■ ACKNOWLEDGMENTS

We thank Stanislav Bellaousov for his assistance with ShapeKnots.

■ ABBREVIATIONS

DMS, dimethyl sulfate; CMCT, 1-cyclohexyl(2-morpholinoethyl)carbodiimide metho-*p*-toluene; NMIA, *N*-methylisotoic anhydride; SHAPE, selective 2′-hydroxyl acylation analyzed by primer extension.

■ REFERENCES

(1) Centers for Disease Control and Prevention (2010) Estimates of deaths associated with seasonal influenza: United States, 1976−2007. *Morbidity and Mortality Weekly Report*, Vol. *59*, pp 1057−1062, Centers for Disease Control and Prevention, Atlanta.

(2) Li, F. C., Choi, B. C., Sly, T., and Pak, A. W. (2008) Finding the real case-fatality rate of H5N1 avian influenza. *Journal of Epidemiology and Community Health 62*, 555−559.

(3) Yu, H., Cowling, B. J., Feng, L., Lau, E. H., Liao, Q., Tsang, T. K., Peng, Z., Wu, P., Liu, F., Fang, V. J., Zhang, H., Li, M., Zeng, L., Xu, Z., Li, Z., Luo, H., Li, Q., Feng, Z., Cao, B., Yang, W., Wu, J. T., Wang, Y., and Leung, G. M. (2013) Human infection with avian influenza A H7N9 virus: An assessment of clinical severity. *Lancet 382*, 138−145.

(4) Jagger, B. W., Wise, H. M., Kash, J. C., Walters, K. A., Wills, N. M., Xiao, Y. L., Dunfee, R. L., Schwartzman, L. M., Ozinsky, A., Bell, G. L., Dalton, R. M., Lo, A., Efstathiou, S., Atkins, J. F., Firth, A. E., Taubenberger, J. K., and Digard, P. (2012) An overlapping protein-coding region in influenza A virus segment 3 modulates the host response. *Science 337*, 199−204.

(5) Lamb, R. A., and Choppin, P. W. (1979) Segment 8 of the influenza virus genome is unique in coding for two polypeptides. *Proc. Natl. Acad. Sci. U.S.A. 76*, 4908−4912.

(6) Lamb, R. A., Lai, C. J., and Choppin, P. W. (1981) Sequences of mRNAs derived from genome RNA segment 7 of influenza virus: Colinear and interrupted mRNAs code for overlapping proteins. *Proc. Natl. Acad. Sci. U.S.A. 78*, 4170−4174.

(7) Wise, H. M., Barbezange, C., Jagger, B. W., Dalton, R. M., Gog, J. R., Curran, M. D., Taubenberger, J. K., Anderson, E. C., and Digard, P. (2011) Overlapping signals for translational regulation and packaging of influenza A virus segment 2. *Nucleic Acids Res. 39*, 7775−7790.

(8) Chen, W., Calvo, P. A., Malide, D., Gibbs, J., Schubert, U., Bacik, I., Basta, S., O'Neill, R., Schickli, J., Palese, P., Henklein, P., Bennink, J. R., and Yewdell, J. W. (2001) A novel influenza A virus mitochondrial protein that induces cell death. *Nat. Med. 7*, 1306−1312.

(9) Wise, H. M., Foeglein, A., Sun, J., Dalton, R. M., Patel, S., Howard, W., Anderson, E. C., Barclay, W. S., and Digard, P. (2009) A complicated message: Identification of a novel PB1-related protein translated from influenza A virus segment 2 mRNA. *J. Virol. 83*, 8021−8031.

(10) Gesteland, R. F., Weiss, R. B., and Atkins, J. F. (1992) Recoding: Reprogrammed genetic decoding. *Science 257*, 1640−1641.

(11) Pelletier, J., and Sonenberg, N. (1988) Internal initiation of translation of eukaryotic mRNA directed by a sequence derived from poliovirus RNA. *Nature 334*, 320−325.

(12) Sperschneider, J., and Datta, A. (2010) DotKnot: Pseudoknot prediction using the probability dot plot under a refined energy model. *Nucleic Acids Res. 38*, e103.

(13) Bellaousov, S., and Mathews, D. H. (2010) ProbKnot: Fast prediction of RNA secondary structure including pseudoknots. *RNA 16*, 1870−1880.

(14) Weeks, K. M. (2010) Advances in RNA structure analysis by chemical probing. *Curr. Opin. Struct. Biol. 20*, 295−304.

(15) Reuter, J. S., and Mathews, D. H. (2010) RNAstructure: Software for RNA secondary structure prediction and analysis. *BMC Bioinf. 11*, 129.

(16) Moss, W. N., Priore, S. F., and Turner, D. H. (2011) Identification of potential conserved RNA secondary structure throughout influenza A coding regions. *RNA 17*, 991−1011.

(17) Hajdin, C. E., Bellaousov, S., Huggins, W., Leonard, C. W., Mathews, D. H., and Weeks, K. M. (2013) Accurate SHAPE-directed RNA secondary structure modeling, including pseudoknots. *Proc. Natl. Acad. Sci. U.S.A. 110*, 5498−5503.

(18) Dirks, R. M., and Pierce, N. A. (2004) An algorithm for computing nucleic acid base-pairing probabilities including pseudoknots. *J. Comput. Chem. 25*, 1295−1304.

(19) Cao, S., and Chen, S. J. (2009) Predicting structures and stabilities for H-type pseudoknots with interhelix loops. *RNA 15*, 696−706.

(20) Wyatt, J. R., Puglisi, J. D., and Tinoco, I., Jr. (1990) RNA pseudoknots. Stability and loop size requirements. *J. Mol. Biol. 214*, 455−470.

DOI: 10.1021/bi501564d
Biochemistry 2015, 54, 3413−3415